Sequential firing codes for time in rodent mPFC

Zoran Tiganj
Department of Psychological and Brain Sciences, Center for Memory and Brain, Boston University, USA

Jieun Kim, Min Whan Jung
Center for Synaptic Brain Dysfunctions, Institute for Basic Science, Daejeon, Korea

Marc W. Howard
Department of Psychological and Brain Sciences, Center for Memory and Brain, Boston University, USA

Abstract

We studied the firing correlates of neurons in the rodent medial PFC during performance of a temporal discrimination task. On each trial, the animal waited for a few seconds in the stem of a T-maze. The firing correlates within a trial gave us a means to assess firing on the scale of seconds. A subpopulation of units fired in a sequence consistently across trials during a circumscribed period during the delay interval. These sequentially activated "time cells" showed temporal accuracy that decreased as time passed as measured by both the width of their firing fields as well as the number of cells that fired at a particular part of the interval. In addition, most units showed gradual changes in their firing rate *across* trials. The time constants of the change in firing were distributed like a power law, with some units showing gradual changes over tens of minutes. The population of time cells showed temporal coding of decreasing temporal accuracy over the scale of a few seconds. Gradual changes across trials could reflect temporal coding over much longer scales as well.

Introduction

A variety of brain regions have been implicated in interval timing over the scale of seconds to minutes, including the striatum (see Buhusi and Meck (2005) for a review) and medial prefrontal cortex (mPFC) (Mangels et al., 1998; Onoe et al., 2001; Kim et al., 2009). Recent evidence has shown that neural ensembles change gradually over periods of time from seconds to minutes in the mPFC (Hyman et al., 2012; Kim et al., 2013); gradual change in ensemble state could be used as a timing signal. For instance, Kim et al. (2013) recently showed that the ensemble state in the medial prefrontal cortex (mPFC) changed gradually during the delay period of a temporal discrimination task. Critically, Kim et al. (2013) found that the discriminability of the time during the delay that could be computed from

the ensemble similarity decreased with time elapsed. Decreasing accuracy with elapsing time is a hallmark of behavioral measures of memory and timing in both human and non-human animals (Lewis and Miall, 2009; Lejeune and Wearden, 2006; Wearden and Lejeune, 2008).

There are many potential mechanisms that could cause a change in accuracy at the ensemble level as time elapses. For instance, a population of neurons whose firing rate changes monotonically as a function of the logarithm of the time during the delay would have this property; Kim et al. (2013) reported a population of units exhibiting just this pattern of results. However, there are other alternatives as well. For instance, several labs have reported "time cells" in the hippocampus that fire during circumscribed parts of a delay period (Pastalkova et al., 2008; Gill et al., 2011; Kraus et al., 2013; MacDonald et al., 2011). Different time cells fire at different times during the interval, enabling a population of time cells to generate a signal that could be used in interval timing. If the width of time cells' firing fields increased with their time of peak firing (Howard et al., 2014; Kraus et al., 2013), then the population of time cells would be less able to distinguish times later in the interval. Similarly, if the density of time fields decreased as a function of time (Kraus et al., 2013), this would have the same consequence.

This paper reports the results of analyses on the data set initially reported in Kim et al. (2013). Kim et al. (2013) noted the existence of cells that fired during circumscribed periods of time during the delay interval (see for instance their Figure 3F). Here we study this phenomenon in more detail to determine if the mPFC contains a significant population of sequentially activated time cells and to determine if these cells code time in such a way that there is decreasing temporal accuracy as a function of time within the delay. In addition, we examined evidence for gradual changes of firing across scales much longer than a single trial, up to tens of minutes.

Methods

Recordings and behavioral procedure

The details of the behavioral task are described in Kim et al. (2013). On each pass through the maze (Figure 1A), the animal waited for a period of time in front of a T-junction (dark shaded area in Figure 1C). To obtain a water reward, the animal had to navigate to one goal when a short time interval (< 3.75 s) was presented, and navigate to the opposite goal when a long time interval (> 3.75 s) was presented. In this study, we analyzed only the data recorded during the delay intervals since in that period there were no behavioral demands on the animals. Recordings were made using tetrodes implanted in mPFC of three rats (Figure 1B).

A total of 993 well isolated single units were recorded. Of these, we eliminated 160 units with mean firing rate < 1 Hz during the waiting intervals. Additionally, in order to restrict our attention to units with spike waveforms that were stable over the recording session we eliminated 10 units with a difference of more than 10% in amplitude from the first to the last 5 min of each session. A total of 723 units contributed to the subsequent analyses.

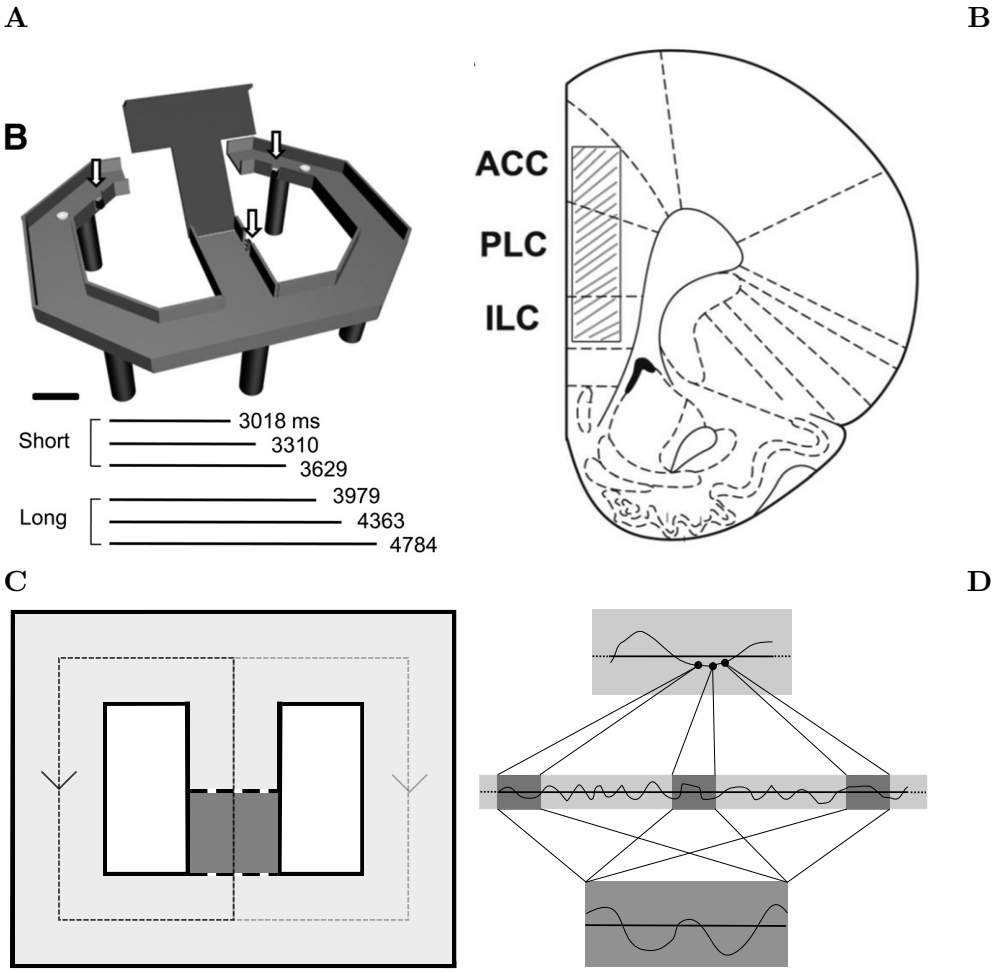

Figure 1. **A.** The maze contained a drawbridge that required animals to wait at a particular location on each trial. If the delay was short, the animal was rewarded for turning one direction at the T; a long delay required a turn in the other direction. **B.** Schematic of recording locations (shaded regions). The diagram is a coronal section view of the brain (2.7 mm anterior to bregma).**A, B** reproduced from Kim et al. (2013). **C.** Temporal bisection task. The animal had to wait for one of six different delay intervals in a limited space (dark gray shaded area), and then navigate through either left or right path (dark gray and light gray dashed lines respectively), depending on the duration of the presented time interval. **D.** The across- and within-trial analysis. The schematic in the middle displays a snapshot of the timeline, represented with a full black line with dots at each end. Dark gray shaded areas are the delay intervals, and light gray shaded areas are the time when the animal was moving through the rest of the maze. The black line is a cartoon example of the firing rate from one cell. All the analysis was done on the neural activity recorded during the delay intervals. In the across-trial analysis (top plot) each delay interval is represented with the mean firing rate, while in the within-trial analysis (bottom plot) neural activity was averaged across all delay intervals.

Analysis across time scales

We examined the firing during delay intervals across two very different time scales (Figure 1D). First, we considered the firing of neurons as a function of time within the delay period. For this analysis we considered only the longest delay interval (almost 5 s). Second, we examined changes in firing from one delay period to the next. Because each delay period was separated by on average 20 s (20 ± 14 s) as the animal traversed back to the waiting location, this analysis allowed us to compare changes in firing over much longer time scales. We analyzed the first 164 trials in each recording session, meaning that we could assess changes in firing up to tens of minutes (164×20 s is more than 50 minutes).

Classification of time cells

Kim et al. (2013) reported a population of units that started firing prior to the initiation of the delay and decreased their firing as the delay proceeded and another population of units that increased their firing monotonically during the delay interval. Both groups could be responding to some event that preceded the delay interval or they could be predicting an event that follows the delay interval. In these analyses we restricted our attention to units that both started and stopped firing within the delay interval on trials in which the animal completed the task successfully. We first processed the data by smoothing the spike train recorded on each trial with a Gaussian-shaped window with 200 ms standard deviation. We then averaged the smoothed activity across correct trials. To be classified as a time cell, units had to satisfy several criteria. First, units had to exhibit an average firing frequency of at least 4 Hz over the delay interval and fire at least one spike in at least 15 different trials. Second, to identify units that showed variability in firing during the delay we required there be at least one time point in the delay interval where the unit's averaged firing rate was no more than 40% of its peak firing rate in the interval. Finally, we required that the unit's firing rate 400 ms before and after the averaged delay interval did not exceed the peak firing rate observed during the interval. The last criterion was set to avoid including cells which firing rate had a general tendency of growth or decay, even outside the delay interval.

Quantifying the time scale of across-trial fluctuations

To quantify long range gradual changes in neural activity we constructed a measure of the duration of each units' autocorrelation across trials. For each unit we took the average firing rates in the delay intervals of the first 164 trials in the recording session. We then computed the autocorrelation function of this time series. We defined the "time constant" of the unit as the time at which the autocorrelation function of the actual data fell within the first standard deviation of the autocorrelations of a surrogate data set constructed from 1000 independent shuffles of the firing rates. This measure can produce time constants as small as zero trials for a unit that is not autocorrelated. Under most circumstances, the method cannot yield time constants longer than 82 trials. In reporting time constants, we multiply the number of trials by the average time of a trial (20 s) to give an intuitive sense of the scale of the autocorrelation.

Estimating distributions using maximum likelihood

Analyses of the within-trial activation generated distributions of the time point at which units were maximally active. Across-trial analyses generated distributions of the time constants across units. In order to characterize the form of these distributions, we fit various models to the distribution. Given a value x, we computed the likelihood $P(x|\theta)$ of that value x given a model parameterized by θ. For each model and each parameterization, we estimated the joint probability of all of the values by taking the sum of the logarithm of the likelihoods. Given that models we considered were either zero parameters (uniform distribution) or one-parameter (exponential and power law distribution) we found the maximum likelihood estimate of the parameter by simply sweeping through all possible values of the parameter. Models with different numbers of parameters were compared using standard methods (AIC and BIC). To estimate a confidence interval on the parameter around the best-fitting value θ_o, we estimated the values θ_- and θ_+ such that

$$\frac{\int_{\theta_-}^{\theta_o} P(\mathbf{x},\theta')d\theta'}{\int_{-\infty}^{\theta_o} P(\mathbf{x},\theta')d\theta'} = \frac{\int_{\theta_o}^{\theta_+} P(\mathbf{x},\theta')d\theta'}{\int_{\theta_o}^{\infty} P(\mathbf{x},\theta')d\theta'} = 0.95,$$

where $\mathbf{x}$ is the entire set of values in the experimental data. The range between θ_- and θ_+ thus contains 95% of the probability mass of the distribution.

Results

Temporal coding on the order of seconds

From the within-trial analysis we identified a subpopulation of sequentially activated units that fired at a consistent, circumscribed time during delay trials (Figure 2). These mPFC units appear to have firing correlates that resemble time cells observed in the hippocampus (Kraus et al., 2013; Gill et al., 2011; MacDonald et al., 2011; Pastalkova et al., 2008; Modi et al., 2014). A total of 122/723 units were classified as time cells.

First, we note informally that the population of time cells decreased in its temporal accuracy as time during the interval proceeds. Figure 3A shows the ensemble similarity (cosine of the normalized firing rate vectors) of the population of time cells between all pairs of time points during the delay period. This finding replicates the conclusions of Kim et al. (2013) but restricting attention to the population of time cells. Further analyses revealed two causes for the decrease in temporal accuracy. These can be read off from Figure 3B, which shows the temporal profile of all 122 units classified as time cells, sorted by their median spike time.

The width of firing fields increased with the passage of time. First, note that the width of the central ridge in Figure 3B increases as one moves from the left of the plot to the right of the plot. This suggests that the units that have elevated firing rate earlier in the delay interval tend to have narrower time fields than the units that fire later in the delay interval. This impression was confirmed by analyses of the across-units relationship between the time of the peak firing rate and widths of the time fields across units. The width was defined as the time that the activity in the averaged delay interval is above the 40% of its peak firing

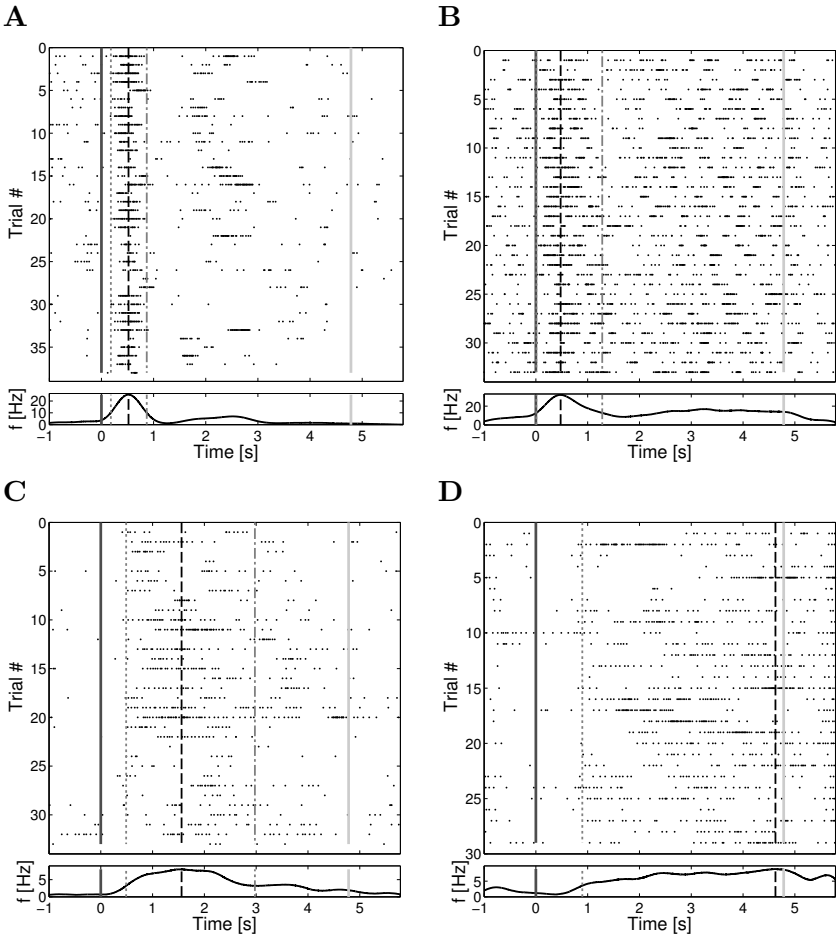

Figure 2. Examples of mPFC time cells that fired consistently across trials during a time window within the delay interval. Each of the four columns (A-D) displays activity of a single cell. The cells are ordered such that width of the time field and the peak time increase progressively from the first to the fourth cell. The top row shows raster plots and the bottom row shows the averaged trial activity. Dark gray and light gray lines mark the start and the end of delay intervals respectively. Gray dotted and dash-dotted lines mark the start and the end of the time fields respectively. Black dashed lines mark the time of the peak firing rate. The activity of the unit in D did not decrease to the threshold level after reaching the peak so only start of the time fields is marked.

rate in the interval. We found weak but significant correlation between the width and the peak time (Pearson's correlation 0.34, $p < .001$).

Later times are represented by fewer cells than earlier times. Second, the population of cells covers the entire delay interval, but not evenly. The number of cells with peak firing later in the interval is smaller than the number of cells with peak firing earlier in the interval. This can be seen from the fact that the central ridge does not follow a straight line, as would have been expected of a uniform distribution of peak times, but flattens as the interval proceeds. To quantify this, we examined the distribution of the peak times. We found the distribution was much more likely assuming a power law distribution than a uniform distribution (ΔAIC=30, ΔBIC=33) and much more likely with a power law distribution than an exponential distribution (ΔLL = 7), meaning that the likelihood of the data given the best-fitting power law distribution was about 1000 times greater than the likelihood of the data given the best-fitting exponential distribution. The best fitting value for the exponent of the power law was $-.41$. The 95% confidence interval did not overlap with zero (-.37 to -.44). This does not provide strong evidence that the "true" distribution is in fact power law rather than some other function with a long tail, but it does compellingly reject the uniform distribution, meaning that more units had time fields early in the delay than later in the delay.

mPFC time cells and ramping cells convey comparable amount of temporal information. We quantified how well the mPFC neuronal ensemble kept track of the elapse of time. The longest time interval (4784 ms) was divided into 10 equal-duration bins and the order of the middle eight bins was decoded based on neural activity within each bin using linear discriminant analysis (Kim et al., 2013). We compared the results on different populations of cells: all 722 cells (Figure 4A), all 122 time cells (Figure 4B) and 122 ramping cells (selected randomly from a total of 228 cells that exhibit ramping firing rate, Figure 4C). The number of selected ramping cells that were also time cells was 66. The mean error in the prediction of elapsed time was similar for all three populations. This suggests that populations of time cells and ramping cells can convey roughly the same amount of information about the elapse of time.

Neither of these findings were an artifact of trial averaging. To confirm that the properties seen in Figure 3 were not simply an averaging artifact, we repeated the analyses, but rather than taking the average smoothed firing rate as input, we took the average of the product of the smoothed firing rate on adjacent trials. In these alternate analyses, only temporally-specific firing that is consistent from one trial to the next contributes to the description of each unit's time field. The findings were qualitatively similar to those from Figure 3. Again there was a significant correlation between time of peak firing and the width of the time field (Pearson's correlation 0.41, $p < .001$). As before, the distribution of time fields was better fit by a power law distribution than by a uniform distribution (ΔAIC=20, ΔBIC=17) and better fit by a power law than by an exponential distribution (ΔLL=8). The best fitting value for the exponent of the power law was $-.39$, close to the value (-.41) found for the actual data. As in the actual data, the 95% confidence interval did not overlap with zero (-.34 to -.43).

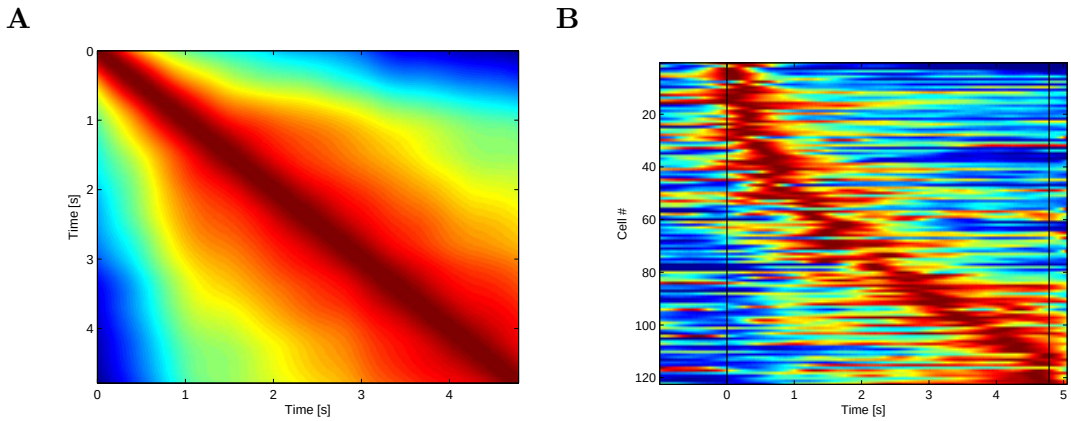

Figure 3. mPFC Time fields show decreasing temporal accuracy for events further in the past. **A.** Ensemble similarity given through a cosine of the angle between normalized firing rate population vectors. The angle is computed at all pairs of time points during the delay period. The bins along the diagonal are necessarily one (warmest color). The similarity spreads out indicating that the representation changes more slowly later in the delay period than it does earlier in the delay period. **B.** Each row on the heatplot displays the firing rate (normalized to 1) for one time cell. White corresponds to high firing rate, while black corresponds to low firing rate. Vertical black lines mark the start and the end of the delay interval. The cells are sorted with respect to the median of the spike time in the delay interval. There are two features related to temporal accuracy that can be seen from examination of this figure. First, time fields later in the delay are more broad than time fields earlier in the delay. This can be seen as the widening of the central ridge as the peak moves to the right. In addition the peak times of the time cells were not evenly distributed across the delay, with later time periods represented by fewer cells than early time periods. This can be seen in the curvature of the central ridge; a uniform distribution of time fields would manifest as a straight line.

Time fields could not be accounted for by observed behavioral correlates. It is possible that units that fire during circumscribed periods of time do so not because of time *per se*, but because of some behavioral state that happens to occur at the same time during each trial. For instance, perhaps the animal adopts a strategy of walking very slowly from one side of the maze to the other at a constant velocity; the animal's location at the time that the interval ends serves as a proxy for time since the interval began.

To determine whether the time cell findings were solely due to behavioral correlates, we repeated the analyses considering only the units that did not show a significant behavioral correlate. The behavioral parameters we had available were position along the x axis, position along the y axis and movement speed. We divided each longest delay interval into 50 bins and computed the mean firing rate for each bin for all the intervals. Firing rate of 48 out of 122 time cells was significantly correlated with at least one of the behavioral parameters (Pearson's correlation coefficient with $p < .01$). Instead of doing the analysis on all 122 time cells we used only 74 behaviorally uncorrelated cells. The findings were qualitatively similar to the results found for all 122 units classified as time cells. Even with relatively low number of cells the time of peak firing and the width of the time field were still correlated (Pearson's correlation 0.27, $p = .018$). The distribution of time fields was better fit by a power law distribution than by a uniform distribution (ΔAIC=7, ΔBIC=5)

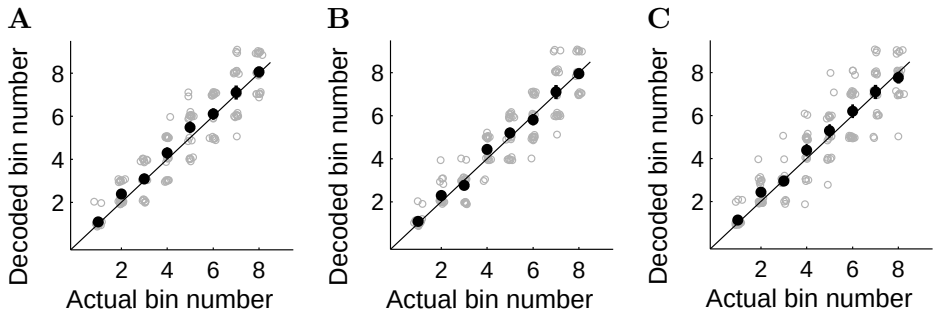

Figure 4. Population of mPFC time cells carried similar amount of temporal information as a same-size population of ramping cells. Decoded bin number versus actual bin number. Open gray circles denote the trial-by-trial decoding results for each bin. Filled black circles and error bars denote their means and SEM across trials. **A.** Temporal decoding based on all 723 reported units. Mean error: 0.71 bins. **B.** Temporal decoding based on all 122 time cells Mean error: 0.59 bins. **C.** Temporal decoding based on the randomly chosen 122 ramping cells. Mean error: 0.70 bins.

and slightly better fit by a power law than by an exponential distribution (ΔLL=1.5). The best fitting value for the exponent of the power law was $-.29$.

Temporal variability in firing across minutes

In addition to the reliable changes in the firing of time cells on the scale of seconds within the delay interval, we also observed gradual changes in the firing properties of many units that changed slowly across trials. Figure 5 shows representative examples. Note that some units increased their firing transiently; others decreased or increased over the entire session. Almost all of the units showed some evidence of autocorrelation across trials. Out of 723 units, 561 showed a time constant of at least one trial. Somewhat reminiscent of the distribution of peak times of the time cells, many more units had short time constants than a long time constants. The distribution of time constants across units was described well by a power law distribution (Figure 6). The power law fit was much more likely than uniform (ΔAIC$>$ 1000, ΔBIC$>$ 1000) and exponential fit (ΔLL = 119). The exponent of the best fitting power law distribution was -1.76 with the 95% confidence interval defined with exponents -1.65 and -1.88.

Across-trial variability was observed in a population that overlapped with within-trial temporal coding. Some units exhibited both within and across-trial gradual changes of the firing rate. The distribution of across-trial time constants for cells classified as time cells did not differ reliably from the distribution of across-trial time constants of all units (K-S test statistic 0.0579).

Across-trial variability could not be attributed to behavioral correlates. We tested whether the gradual changes in the neural activity are caused by any of the available behavioral correlates. As in the earlier analysis on the time cells, behavioral correlates were position along the x axis, position along the y axis and movement. Two pieces of evidence argue against the hypothesis that the long time constants we observed were attributable to behavioral correlates.

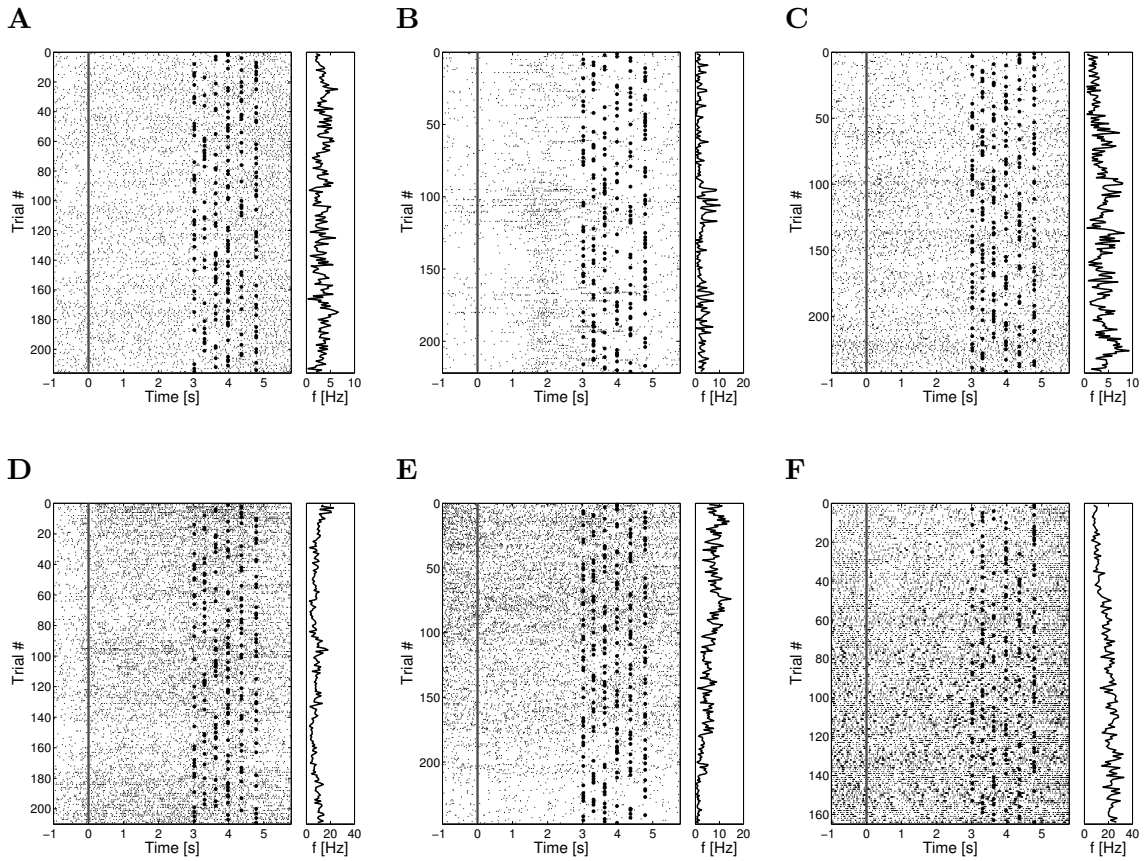

Figure 5. Examples of units that gradually changed their firing rate across trials. Each raster plot is aligned on the start of the waiting period of each trial (gray line). The end of the interval is marked by a large black dot. The plot on the right shows firing rate during the delay period as a function of trial number. The start of each trial was separated by approximately 20 s. The time constants of the six units were A: 280 s; B: 340 s; C: 380 s; D: 440 s; E: 740 s; F: 940 s.

First, the measured behavioral correlates were autocorrelated over much shorter time scales than the neural data. Neural changes were quantified through a time constant derived from the autocorrelation function of firing rate. Therefore, we computed an analogous measure for the behavioral data. Distributions of the time constants were, for each of the three behavioral correlates significantly different than the distribution coming from the neural data (K-S test, $p < 0.001$). Behavioral time constants were on average about five times shorter than neural time constants.

Second, if behavior was causing the autocorrelation observed in the units, because behavior is the same for all units recorded in the same session, we would expect to see units from the same session to have time constants that are correlated with one another. In contrast, if behavior was not a major factor in causing across-trial changes in firing, then units from the same session would have the same statistics as units recorded from different sessions. This hypothesized correlation in time constants should manifest as a change in the distribution across sessions of mean time constants for units within a same session. To test

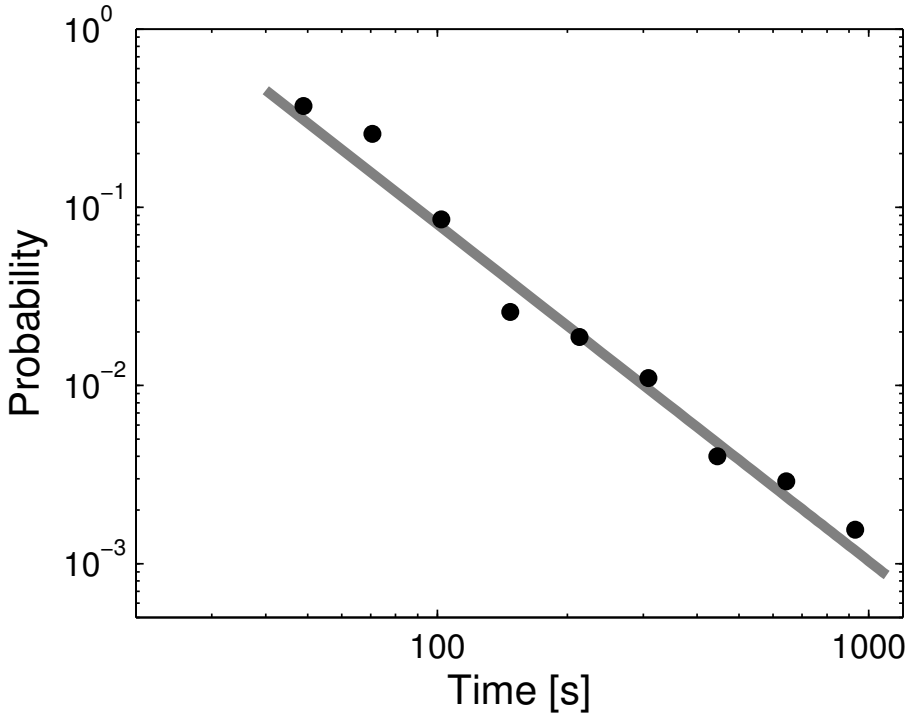

Figure 6. The distribution of time constants across units approximates a power law distribution. For each unit, a time constant of across-trial firing was estimated from its autocorrelation (see text for details). The time constant measured in number of trials was then multiplied by the average time between trials (20 s) in order to provide a sense of the scale of the fluctuations. The black dots show the probability density function of the data on log-log paper. The gray line gives the maximum likelihood power law fit. The exponent of the power law is -1.76.

this hypothesis, we computed F statistics from the time constants of all 722 units, treating the session identity as a categorical variable. Since the time constants are not normally distributed, to evaluate whether there is significant correlation between the time constants and the sessions identities we shuffled the unit identity with respect to recording sessions for 1000 time and computed F statistics for each shuffle. Rank of the observed data within the shuffled data was 627, suggesting that units that were recorded in a same session were not more likely to have a particular time constant.

Discussion

This study shows that mPFC contains sequentially activated time cells, similar to those previously reported in the hippocampus. The time fields of these units spanned the entire 5 s delay interval, but with temporal accuracy that decreased as the delay elapsed. The width of the time fields increased with temporal distance from the onset of the delay period and distribution of the firing rate peaks strongly deviated from the uniform such that more units represented time periods early in the delay rather than later in the delay. Additionally, neurons in mPFC exhibited gradual changes in firing across trials spanning up to at least tens of minutes. The number of units that exhibited a particular time constant

decreased as a power law function of the duration. Taken together, these results suggest that mPFC could be used for timing over a variety of time scales from a few hundred milliseconds up to tens of minutes.

Could these findings be recording artifacts

The results in this paper are consistent with, but do not uniquely specify, the hypothesis that firing of mPFC neurons maintain a temporal memory over a variety of time scales. One alternate possibility is that the temporally modulated firing reflect some other factor that also changes over time. Temporally-correlated behavior is one candidate; recording artifacts are another.

The behavioral measures that were measured in this experiment (x-position, y-position and running speed) were not sufficient to account for either the within-trial or the across-trial temporal modulation. However, this does not exclude the possibility that there are other behavioral factors that were not measured. For instance, it is possible that some animal's might have engaged in some subtle behavioral strategy within each trial, such as shifting weight or some pattern of whisking, that was not measured. Over the course of the session, we would expect the animals to get progressively less thirsty, or for body temperature to change due to exertion. However, we saw across-trial changes across a range of time scales, and cells that both increased and decreased their firing. As a result it is not likely that a single behavioral correlate could cause the gradual change across time scales.

There are a number of factors that could result in artifactual changes in spike-sorting over time on the scale of time within a trial and also across trials. For instance, when a neuron fires repeated action potentials over hundreds of milliseconds, the waveform might change. Alternatively, tetrodes might shift gradually over the recording session. We reduced the possibility that the results are influenced by recording artifacts by eliminating 10 units which average spike waveforms significantly changed during the recording, but there is no way to know with certainty that the results are not attributable to some recording artifact. However, similar findings have been observed with calcium imaging in the hippocampus, which would not be subject to the same set of recording artifacts. Modi et al. (2014) found time cells that fire during a circumscribed part of the delay period of a trace conditioning experiment. Ziv et al. (2013) showed that the hippocampal representation of place on a simple linear track changed gradually across days.

Relationship to temporally-modulated firing in the hippocampus

This paper reports that mPFC contained sequentially activated time cells with decreasing temporal accuracy and cells that changed their firing gradually over long periods of time. Both of these phenomena have previously reported in the hippocampus. For instance, several studies have found evidence for hippocampal cells that fire during circumscribed periods of time within a delay interval (Gill et al., 2011; Kraus et al., 2013; MacDonald et al., 2011; MacDonald et al., 2013; Modi et al., 2014; Naya and Suzuki, 2011; Pastalkova et al., 2008). Some of these studies have found evidence for decreasing temporal accuracy as a function of delay, due to spread in time field width (Howard et al., 2014; Kraus et al., 2013) or due to a non-uniform distribution of time field locations (Kraus et al., 2013). In addition, gradual changes in firing across minutes have been observed in the human (Howard et al., 2012) and rat hippocampus (Mankin et al., 2012;

Manns et al., 2007). However, these studies have characterized gradual change at the population level; it is not yet clear whether the hippocampus also shows a power law distribution of time constants like we observed in the mPFC and, if so, whether the exponent corresponds.

It is also not clear in either the mPFC or the hippocampus whether the gradually-changing firing carries meaningful information about past events or not. This could be established (and recording artifacts definitively ruled out) if an experiment were to demonstrate control over gradually changing firing. For instance, the unit in Figure 5E decreases its firing around trial 80 and then decays gradually over about 50 trials, extending a few hundred seconds. Even if we were able to identify some unusual event that occurred around trial 90, this would not demonstrate causal control over the cell's firing. In order to do so, we would have to present the hypothetical stimulus multiple times, separated by a few hundred seconds and show that the stimulus consistently causes the same profile of firing. Examining recordings from monkeys, Bernacchia et al. (2011) showed that gradual changes in the firing of neurons in a variety of regions, including prefrontal cortex, reflected the history of reward, so it is at least possible in principle for the brain to maintain information about some past events over long periods of time.

Concluding remarks

Previous work has shown that neural ensembles in the rodent mPFC code for time with decreasing temporal accuracy (Kim et al., 2013) and change gradually over long periods of time (Hyman et al., 2012). This paper extends these findings in two ways. First, a subpopulation of units in the mPFC fired like sequentially activated time cells, firing for circumscribed periods of time during the delay of an interval discrimination task. These time cells exhibited decreasing temporal accuracy in two ways. First, time cells that fired later in the delay interval had wider temporal receptive fields than time cells that fired earlier in the delay. Second, the distribution of time fields was not uniform. More cells had time fields earlier in the delay period than later in the delay period. In addition to these findings regarding firing correlates while timing delays on the order of seconds, we also observed gradual changes in firing rate over time scales up to a thousand seconds (Hyman et al., 2012). The gradual change across the population was attributable to units that showed autocorrelation at different time scales. Most units showed at least some significant autocorrelation across trials, which were separated by on average 20 s. A few units showed autocorrelations across the entire session, lasting tens of minutes. The distribution of time constants across units was well-described by a power law distribution. Taken together, these findings are consistent with the hypothesis that the mPFC is part of a system that represents time with decreasing accuracy over a range of time scales from a few hundred milliseconds up to thousands of seconds.

References

Bernacchia A, Seo H, Lee D, Wang XJ (2011) A reservoir of time constants for memory traces in cortical neurons. *Nature Neuroscience* 14:366–72.

Buhusi CV, Meck WH (2005) What makes us tick? Functional and neural mechanisms of interval timing. *Nature Reviews Neuroscience* 6:755–65.

Gill PR, Mizumori SJY, Smith DM (2011) Hippocampal episode fields develop with learning. *Hippocampus* 21:1240–9.

Howard MW, Viskontas IV, Shankar KH, Fried I (2012) Ensembles of human mtl neurons "jump back in time" in response to a repeated stimulus. *Hippocampus* 22:1833–1847.

Howard MW, MacDonald CJ, Tiganj Z, Shankar KH, Du Q, Hasselmo ME, Eichenbaum H (2014) A unified mathematical framework for coding time, space, and sequences in the hippocampal region. *Journal of Neuroscience* 34:4692–707.

Hyman JM, Ma L, Balaguer-Ballester E, Durstewitz D, Seamans JK (2012) Contextual encoding by ensembles of medial prefrontal cortex neurons. *Proceedings of the National Academy of Sciences USA* 109:5086–91.

Kim J, Jung AH, Byun J, Jo S, Jung MW (2009) Inactivation of medial prefrontal cortex impairs time interval discrimination in rats. *Frontiers in Behavioral Neuroscience* 3.

Kim J, Ghim JW, Lee JH, Jung MW (2013) Neural correlates of interval timing in rodent prefrontal cortex. *Journal of Neuroscience* 33:13834–47.

Kraus BJ, Robinson n RJ, White JA, Eichenbaum H, Hasselmo ME (2013) Hippocampal "time cells": time versus path integration. *Neuron* 78:1090–101.

Lejeune H, Wearden JH (2006) Scalar properties in animal timing: conformity and violations. *Quarterly Journal of Experimental Psychology* 59:1875–908.

Lewis PA, Miall RC (2009) The precision of temporal judgement: milliseconds, many minutes, and beyond. *Philosophical Transcripts of the Royal Society London B: Biological Sciences* 364:1897–905.

MacDonald CJ, Carrow S, Place R, Eichenbaum H (2013) Distinct hippocampal time cell sequences represent odor memories immobilized rats. *Journal of Neuroscience* 33:14607–14616.

MacDonald CJ, Lepage KQ, Eden UT, Eichenbaum H (2011) Hippocampal "time cells" bridge the gap in memory for discontiguous events. *Neuron* 71:737–749.

Mangels JA, Ivry RB, Shimizu N (1998) Dissociable contributions of the prefrontal and neocerebellar cortex to time perception. *Cognitive Brain Research* 7.

Mankin EA, Sparks FT, Slayyeh B, Sutherland RJ, Leutgeb S, Leutgeb JK (2012) Neuronal code for extended time in the hippocampus. *Proceedings of the National Academy of Sciences* 109:19462–7.

Manns JR, Howard MW, Eichenbaum HB (2007) Gradual changes in hippocampal activity support remembering the order of events. *Neuron* 56:530–540.

Modi NM, Ashesh DK, Bhalla SU (2014) CA1 cell activity sequences emerge after reorganization of network correlation structure during associative learning. *eLife* 3.

Naya Y, Suzuki W (2011) Integrating what and when across the primate medial temporal lobe. *Science* 333:773–776.

Onoe H, M. K, Onoe K, Takechi H, Tsukada H, Watanabe Y (2001) Cortical networks recruited for time perception: A monkey positron emission tomography (pet) study. *NeuroImage* 13:37 – 45.

Pastalkova E, Itskov V, Amarasingham A, Buzsaki G (2008) Internally generated cell assembly sequences in the rat hippocampus. *Science* 321:1322–7.

Wearden JH, Lejeune H (2008) Scalar properties in human timing: conformity and violations. *Quarterly Journal of Experimental Psychology* 61:569–87.

Ziv Y, Burns LD, Cocker ED, Hamel EO, Ghosh KK, Kitch LJ, El Gamal A, Schnitzer MJ (2013) Long-term dynamics of ca1 hippocampal place codes. *Nature Neuroscience* 16:264–6.